

CALIBRATING THE ULTRACAM AERIAL CAMERA SYSTEMS, AN UPDATE

R. Ladstädter^a, H. Tschemmerneegg, M. Gruber

Microsoft Photogrammetry, Anzengrubergergasse 8, 8010 Graz, Austria

^arichard.ladstaedter@microsoft.com

KEY WORDS: Digital Camera, Camera Calibration, Stitching

ABSTRACT

We present the method of the geometric calibration of the digital camera systems UltraCam X(p) and UltraCam L. The entire process consists of three major steps: the laboratory calibration, the stitching process and the self calibration process. The laboratory calibration was implemented in early 2003 and did not change much until today. It is based on a highly redundant set of images from a 3D calibration target. The initial calibration data set is computed by means of a least squares bundle adjustment with specific parameters. These parameters provide the basic geometric description of the sensor. The stitching process is the basic concept during the post processing of each frame taken by our camera systems. The transformation of each layer of the multi cone design into one single image coordinate system has been improved and the latest status of this methodology is presented within this contribution. The self calibration process is the final step of the geometry chain. We show the implementation in our UltraMap AT software product and present results from an UltraCam L flight mission.

INTRODUCTION

The geometric quality of UltraCam images depends on three major steps:

1. The initial calibration in a 3D test field.
2. Stitching of the image parts to a full frame virtual image (part of the image post-processing).
3. Self calibration in the bundle adjustment.

All of these steps have been presented in detail in previous papers (e.g. Kröpfl et al., 2004; Gruber & Ladstädter, 2006/2008). In this paper, some minor changes of the laboratory calibration are described. The major change however happened in the image post-processing step: a new stitching algorithm has been developed which is not only capable of improving the accuracy and robustness of the stitching result but, in case of an UltraCam Xp system, also allows to validate the underlying calibration data.

In addition, the new medium format camera system UltraCam L will be described, which has quite different geometric properties compared to an UltraCam Xp system (cp. Gruber & Wiechert, 2009). It will also be outlined how the UltraCam L benefits from the new calibration and stitching methods.

Finally, the aerial triangulation software package UltraMap-AT is shortly introduced and the self

calibration capabilities in the bundle adjustment are described.

LABORATORY CALIBRATION

Calibration of all UltraCam camera models (including UltraCam L) is performed in the Vexcel calibration lab (3D test field) in the basement of the Microsoft Photogrammetry office building in Graz. Two improvements of the calibration workflow have to be mentioned:

1. Recording of sensor temperatures at calibration time, stored with calibration data (starting with the UCXp series).
2. Estimation of the relative rotation of all camera cones with respect to the master cone, epipolar transformation is stored to pre-correct layer images (starting with the UltraCam L series).

The recording of the calibration temperature is an important step to make the TDM corrections more robust, i.e. independent from the image content. The difference dC between the temperature at calibration time and at flight time can now be directly deduced from the measured sensor temperatures (cp. Fig. 1). An estimation of dC from the stitching scales is no longer necessary (this is also not possible anymore for the UltraCam L camera system).

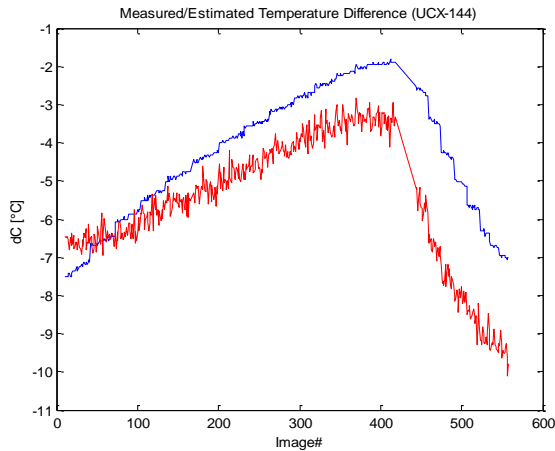


Fig. 1: Measured temperature difference (blue) vs. estimated dC (red).

The second improvement concerns the consideration of the relative orientation of all cones with respect to the master cone ('platform calibration'). Due to the syntopic exposure of the PAN cones, an epipolar transformation allows to rectify all image layers beforehand the actual stitching process. This is of special importance for the UltraCam L camera model, because there is no dedicated master cone as for the UltraCam X(p) series.

IMAGE POST PROCESSING

The raw images of in total 13 CCD sensors of an UltraCam X(p) system are stored as Level0 image data. During image post-processing (Level0 to Level2) those sensor images have to be stitched together to form a geometrically correct virtual (full frame) image. In the previous versions of the UltraCam post-processing software OPC the following steps have been performed by the stitching algorithm:

1. Formation of image layers for each cone, i.e. transformation of the sensor images into the layer coordinate system of each cone using the calibrated sensor positions and applying a correction grid (LUT) to correct for non-linear errors.
2. Matching of tie points in the small overlap regions between the nine PAN sensors.
3. Calculation of 2D projective (8 parameter) transformations between layers 1, 2 and 3 onto layer 0 (master cone image).
4. Resampling of the virtual PAN image using the layer transformations.
5. Matching of tie points between the virtual PAN image and the green colour image and between the four colour layers (R,G,B and NIR).
6. Registration of the colour layers onto the virtual PAN image by 2D projective transformations.

This basic stitching algorithm has been improved by a so called "temperature dependant model" (TDM), which corrects for systematic sensor drift caused by the offset of the camera temperature between calibration time and production flight (see Ladstädter, 2007). This has been the first important step to consider the camera calibration to be not absolutely stable but to undergo changes during a flight mission (described by TDM).

The main differences of the new stitching algorithm implemented in the new UltraMap v2.0 release are as follows:

1. In addition to the tie points matched between the PAN sensors, tie points are also matched between each PAN sensor and the green colour channel (colour master). In this way the number of tie points used for PAN stitching is increased by a factor of 2-3 and tie points are well distributed over the whole virtual image plane (VIP).
2. The initial formation of image layers based on the camera calibration is omitted. Layer transformations are complemented by individual similarity (S-) transformations of each sensor image. This concept is more flexible than the previous stitching method and is called 'free image mosaicking'.
3. The optimal reconstruction of the inner orientation of the virtual PAN image is guaranteed by a similarity transformation of the free adjusted PAN mosaic onto the calibrated sensor positions of the master cone.

Fig. 2 shows both the tie points extracted in the 12 overlapping regions of the nine PAN sensors (P/P tie points) and the tie points matched between each PAN sensor and the green colour channel (P/C tie points) in a single UltraCam Xp image. For a well textured image, about 10.000 P/P tie points and 17.000 P/C tie points can be expected. Note, that the green colour channel has a three times lower resolution than the PAN channel, so the accuracy of the P/C tie points is reduced by this factor. On the other hand, the whole virtual image plane is covered by one monolithic sensor which results in a very stable geometric quality of the P/C tie points. Therefore, by the use of P/C tie points, the quality of the stitching algorithm is improved in two ways:

1. The robustness is increased because of the high number and well distribution of the additional tie points. Even in low textured images (e.g. flown over sea or desert areas) we can still expect a sufficient number of P/C tie points. Stitching problems caused by missing P/P tie points in one or more PAN

overlaps can therefore be avoided to a great extent.

2. The accuracy of the stitching result is also increased, because the algorithm benefits from the stable geometric properties and the even distribution of the P/C tie points.

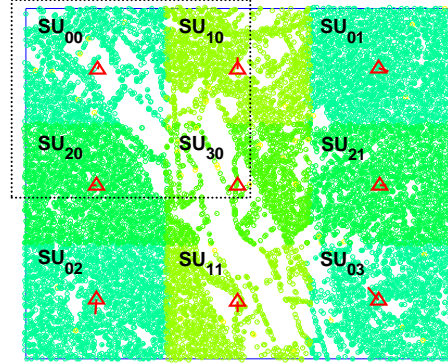
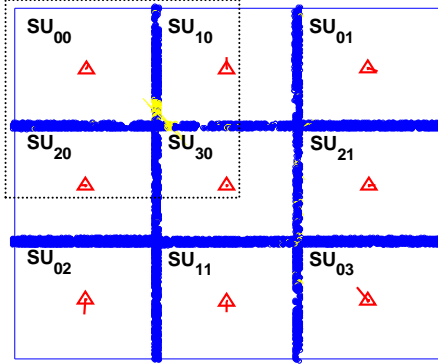


Fig.2: Distribution of the P/P tie points (left) and the P/C tie points (right) in the VIP. Positions of the nine PAN sensors (SU_{ij}) are marked by red triangles. The area marked by the dashed rectangle is enlarged in Fig 3 and 4.

The basic idea of the new stitching core is to compose a virtual PAN mosaic free from systematic deformations caused by eventually inaccurate or even invalid calibration data (e.g. caused by mechanical stress). This algorithm, called ‘free image mosaicking’ will now be described in more detail.

Each of the nine PAN sensors is transformed individually into the specific image layer using S-transformations (4 parameters: shift_x, shift_y, rotation, scale). The image layer is then transformed into the VIP using a 2D projective transformation (8 parameters) to compensate for differential motions of the camera between the syntopic exposure of the PAN cones. For the transformation of an P/P tie point (index k) measured in the sensor coordinate system $u_{i,j}$ of the sensor j on layer i into the camera coordinate system x^{VIP} defined in the VIP, the following basic equation can be given:

$$(1) \quad x_{i,k}^{VIP} = P_i \cdot S_{i,j} \cdot u_{i,j,k}$$

The matrix P_i holds the projective transformation from layer i to the virtual image plane (layer transformation) and S represents the similarity transformation from the sensor into the specific layer (sensor transformation). To avoid over-parameterisation, depending on the image layer (=cone), some parameters have to be fixed and/or additional constraints (AC) have to be applied (see table 1).

The determination of stitching parameters is improved e.g. by the de-correlation of the scale and shift parameters. Furthermore, the number of parameters can be (slightly) increased which allows for better modelling of the stitching process.

Layer	#Sensors	Fixed parameters / add. constraints	#Parameters	DOF
0	4	P_0 / 4 AC	$4 \times 4 = 16$	12
1	2	4 AC	$2 \times 4 + 8 = 16$	12
2	2	4 AC	$2 \times 4 + 8 = 16$	12
3	1	S_3	8	8
G	1	S_G	8	8
Total:			64	52

Table 1: Parameters and DOF of the free mosaicking algorithm (UCX)

As it can be seen from table 1, the coordinate systems of the virtual image plane and the master cone (layer 0) are identical (P_0 is set to the unit transformation). Three additional constraints (AC) are used to guarantee an optimal reconstruction of the inner orientation of the PAN mosaic (see section below). For layers 1 and 2, four additional constraints are used. Layer 3 and the green colour channel (G) are single sensor cones, which means that sensor and layer transformations cannot be separated (the sensor transformation is therefore fixed). Note, that by the last transformation, the low resolution green colour channel is registered onto the PAN mosaic. In total, 64 parameters have to be computed in the iterative adjustment procedure (32 in the previous stitching method), but the system has only 52 degrees of freedom (DOF).

Linearization of equation (1) with respect to all of the n parameters involved yields:

$$(2) \quad \tilde{x}_{i,k}^{VIP} + v_k = (P_i) \cdot (S_{i,j}) \cdot u_{i,j,k} + \sum_{l=1}^n \frac{\partial x_{i,k}^{VIP}}{\partial p_l} dp_l$$

Homologue tie points measured on layers $i=a$ and $i=b$ respectively have to coincide after their transformation into the VIP. Therefore, the following constraint can be formulated for the adjusted position \tilde{x} of tie point k in the VIP:

$$(3) \quad \tilde{x}_k^{VIP} = (x_{a,k}^{VIP}) + dx_{a,k}^{VIP} + v_{a,k}^x = (x_{b,k}^{VIP}) + dx_{b,k}^{VIP} + v_{b,k}^x$$

This is re-formulated to obtain equation (4):

$$(4) \quad (x_{a,k}^{VIP}) - (x_{b,k}^{VIP}) + v_{a,k}^x - v_{b,k}^x = dx_{b,k}^{VIP} - dx_{a,k}^{VIP}$$

Finally, two observations (x- and y-component) per tie point can be used in the adjustment:

$$(5) \quad x_{a,k}^{VIP} - x_{b,k}^{VIP} + w_k^x = \sum_{l=1}^n \frac{\partial x_{b,k}^{VIP}}{\partial p_l} \cdot dp_l - \sum_{l=1}^n \frac{\partial x_{a,k}^{VIP}}{\partial p_l} dp_l$$

$$y_{a,k}^{VIP} - y_{b,k}^{VIP} + w_k^y = \sum_{l=1}^n \frac{\partial y_{b,k}^{VIP}}{\partial p_l} \cdot dp_l - \sum_{l=1}^n \frac{\partial y_{a,k}^{VIP}}{\partial p_l} dp_l$$

For the first iteration, all sensors are placed on their calibrated position. This means that the S-transformations determined during camera calibration are used to initialize the parameter set. With the new calibration method described earlier in the calibration section we can also initialise the layer transformations in advance and thus pre-correct layers 1,2 and 3 before the iterative mosaiking algorithm starts.

After transformation of the tie points measured in the nine PAN images and the green colour channel into the VIP, we can calculate residual vectors for the homologous point measurements (see Fig. 3). By adjusting positions, orientations and scales of each sensor involved, the tie point residuals are minimized. Note that different weights are used for the P/P and P/C tie points respectively because those measurement groups represent different levels of accuracy.

The adjustment quickly converges, so after only three iterations we get an excellent result (see Fig. 4). As we can see from the right figure, there is no systematic error left in this area which covers four PAN sensors (nor in the other parts of the PAN mosaic). Outliers (yellow lines) can easily be detected and eliminated from the adjustment (see Fig. 4, left side).

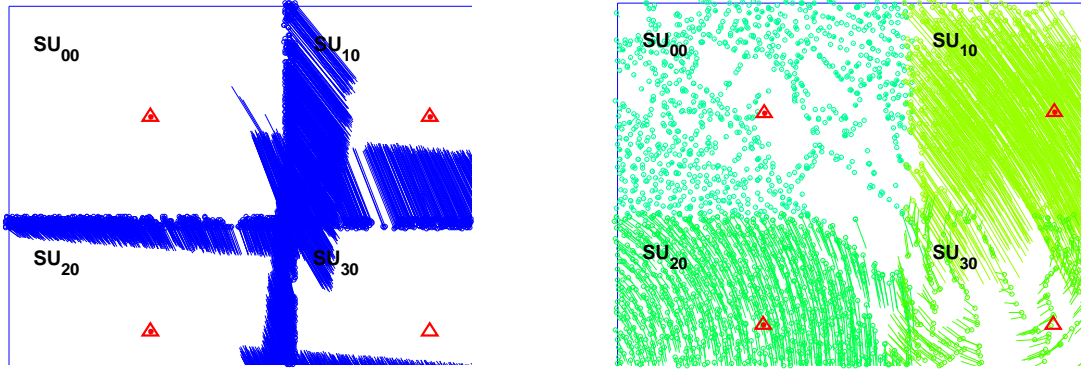


Fig. 3: Residuals of P/P tie points (left) and P/C tie points (right) in the first iteration.

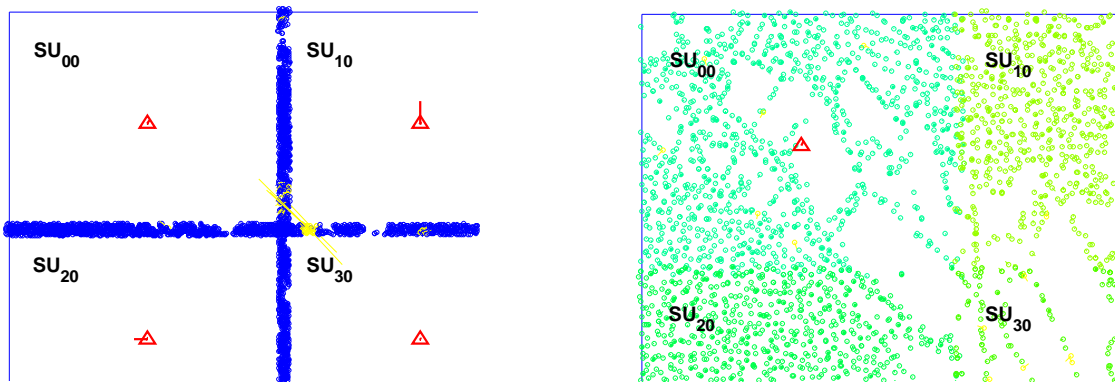


Fig. 4: Residuals of P/P tie points (left) and P/C tie points (right) after three iterations.

OPTIMAL IO RECONSTRUCTION

So far, no calibration information was used in the stitching algorithm (only for initialization). The image mosaic has optimal internal accuracy but is not referenced to the camera coordinate system.

In geodesy, a similar problem has to be solved in a network adjustment. The high internal accuracy of the network is achieved by precise distance and angle measurements, but the network has to be referenced to a given coordinate system, realized by control points of sometimes quite low accuracy (datum problem). Meissl (1962, 1969) has investigated this problem and has given a solution to preserve the high internal network accuracy and to find the optimal solution of the datum problem by an S-transformation as well. This method is now commonly known as “free network adjustment”.

The principle of a free network adjustment is now applied to achieve an optimal reconstruction of the inner orientation of images of an UltraCam X(p) camera system. As mentioned before, an S-transformation of the mosaiked image onto the calibrated sensor positions of the mastercone has to be performed. This is done simultaneously in the iterative adjustment by adding the following constraints on the shift parameters of the master cone sensors:

$$(6a) \quad \sum_{j=1}^4 dx_j = 0; \quad \sum_{j=1}^4 dy_j = 0$$

$$(6b) \quad \sum_{j=1}^4 (x_j^c dx_j + y_j^c dy_j) = 0$$

$$(6c) \quad \sum_{j=1}^4 (-y_j^c dx_j + x_j^c dy_j) = 0$$

By the constraints (6a), a systematic shift of the PAN mosaic with respect to the calibrated sensor positions x_j^c is avoided. Constraint (6b) prevents a systematic scale error and constraint (6c) a systematic rotation (see fig. 5 a-c). By adding those four additional constraints, the residuals between calibrated and adjusted sensor positions will be minimized (cp. Fig. 5d). This method guarantees an optimal reconstruction of the camera coordinate system in the VIP and thus of the inner orientation of the camera system.

Analysing the residuals in the master cone allows to evaluate whether the camera calibration is still valid or not. It is even possible to determine a single displaced sensor, which might have been dislocated e.g. by mechanical stress. Because of the independent image mosaiking process however, displaced sensors will not affect image geometry any more. This is a clear advantage over common stitching algorithms using fixed (calibrated) sensor positions.

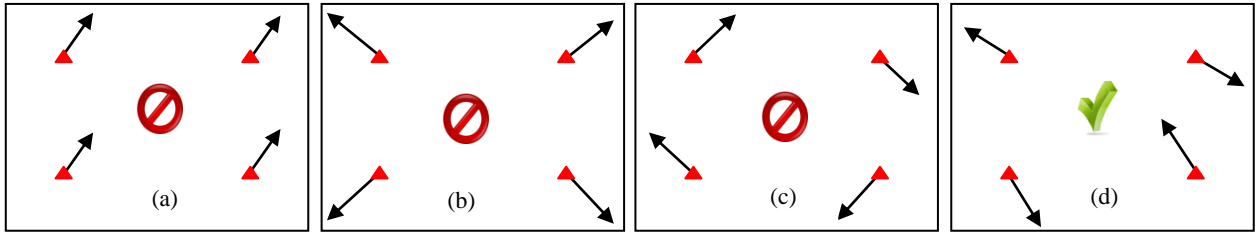


Fig. 5: Residuals between adjusted and calibrated sensor positions (in red) in the master cone.

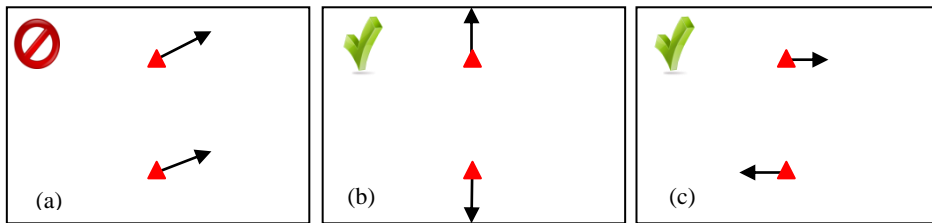


Fig. 6: Residuals between adjusted and calibrated sensor positions in a double sensor cone (e.g. layer 1).

For a double cone (containing two sensors), not all of the constraints (6) can be used (see Fig. 6). A relative differential movement of the sensors should be possible, so only constraints (6a) should be applied (prevent systematic shift of both sensors, see Fig. 6a). However, sensor shifts shown in Fig.6b and c might also be caused by applying a scale or rotation respectively to the layer.

In order to avoid correlation between scale and rotation parameters of the sensor and layer

transformation, the following additional constraints have to be applied:

$$(7a) \quad \sum_{j=1}^2 ds_j = 0$$

$$(7b) \quad \sum_{j=1}^2 dr_j = 0$$

By these constraints, only the relative scaling and rotation of the two sensors might change, any systematic scaling or rotations will go into the layer transformation.

ULTRACAM L MEDIUM FORMAT CAMERA

Vexcel Imaging announced UltraCamL in July 2008 and started to deliver in May 2008. The sensor head is based on 4 camera heads, one for true colour RGB, one for near Infrared and two heads for the panchromatic high resolution image of 64 Megapixels (92 Megapixels for UltraCam Lp). This so called large medium format mapping camera addresses the smaller segment without sacrificing any image quality. Its unique camera design utilizes the concept of the large format camera system UltraCamX(p) for the medium format market. Further noticeable is the compact design. All computing and on board data storage components are integrated into the sensor head (see fig. 7)



Fig. 7: UltraCam L sensor head and integrated data capture and data processing unit.

By that, an affordable integrated and compact mapping solution with a very high productivity became now available to the remote sensing market. The UltraCamL/Lp provides the same geometric accuracy, the same radiometric dynamic, the same mapping and photogrammetric capability and the same forward motion compensation by TDI than the large format cameras but it comes in a medium format package and price.

The RGB cone acquires the colour information to colour the pixels of the PAN image by the well know pan-sharpening methodology with an industry leading ratio of 1:2. The NIR cone collects NIR imagery with the same resolution than the RGB cone to support classification work. The PAN cones are lined up in flight direction and utilize the syntopic exposure for parallax free imagery.

For the UltraCam L camera system, the new stitching method using additional colour tie points had been implemented in UltraMap from the beginning. The algorithm has only been adapted to the reduced number of cones and sensors. Fig. 8 shows how the virtual PAN mosaic is composed of the images of the PAN sensors SU_{00} and SU_{10} which are mounted in separated cones. Only a single overlap exists between these two sensors, which would not allow for a projective 8-parameter transformation of layer 1. This is only possible because of the additional P/C tie points distributed over the whole VIP.

Layer	#Sensors	Fixed parameters / add. constraints	#Parameters
0	1	P_0 / S_0	0
1	1	S_1	8
G	1	S_G	8
			Total: 16

Table 2: Parameters and DOF of the free mosaiking algorithm (UCL)

Table 2 lists the number of parameters used in the PAN stitching algorithm. Note that layer 0 (the left sensor) is considered to be the 'master cone', so the layer transformation is set to the unit transformation. Additional constraints for IO reconstruction cannot be applied (as for an UCX), because both PAN cones are single sensor cones. Therefore the sensor transformations of the PAN cones as well for the green colour cone have to be fixed.

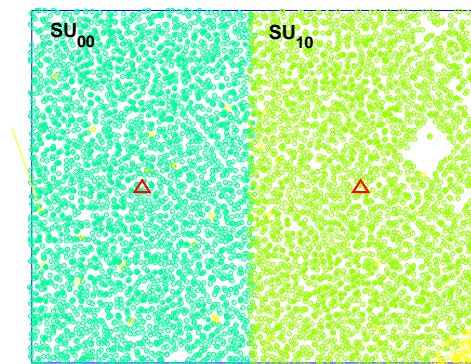
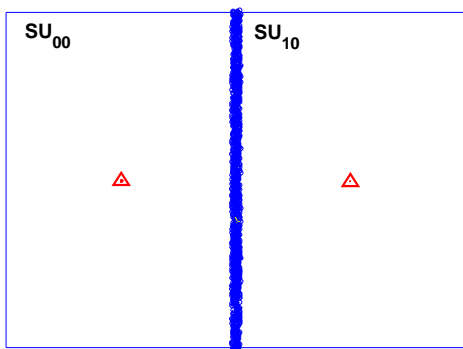


Fig. 8: P/P tie points (left) and P/C tie points (right) of an UltraCam L camera system.

ULTRACAM L PROJECT REVIEW

An UltraCam L flight mission was used to prove the quality of the camera as well as the calibration and geometric post processing results. The mission was carried out in a well known area equipped with ground truth. GPS/IMU data were recorded and added to the adjustment. The entire mission consists of 296 frames, six flight lines north-south and 3 additional cross strips (see Fig. 9). The images of the test project have been processed twice using UltraMap AT:

1. With an experimental stitching algorithm which uses only P/P tie points collected in the single PAN overlap and a reduced (4 parameter) layer transformation. This was done to show how the geometric quality of the stitched PAN image decreases without use of the C/P tie points. In addition, no pre-correction of the PAN layers using the new calibration data was done.
2. The regular stitching algorithm was applied using P/P and P/C tie points. Image layers have been pre-corrected using the epipolar transformation stored in the calibration data.

Remaining systematic image residuals can be analysed after bundle adjustment using the IMPLO tool of BINGO (Kruck, 1984). Note that for both projects, only two additional parameters (correcting for radial distortion) have been used in the bundle adjustment. In fig. 10, left side, the result of the experimental (PAN only) stitching algorithm is shown. As it had to be expected, systematic image residuals in the range of $2\mu\text{m}$ can be observed which are caused by projective distortions of layer 1 with respect to layer 0.

The result of the second run using C/P tie points as well as the layer pre-correction is shown in Fig.10, right side.

There are almost no systematic image residuals visible any more, which proves the new stitching concept presented in this paper and the latest improvements in the calibration procedure.

The overall accuracy level of the final aero-triangulation project is documented by the RMSE value of the image measurements ($0.7\ \mu\text{m}$ for x and y) as well as the remaining GCP residuals of 0.3 Pixel in planimetry and 0.36 Pixel in altimetry.

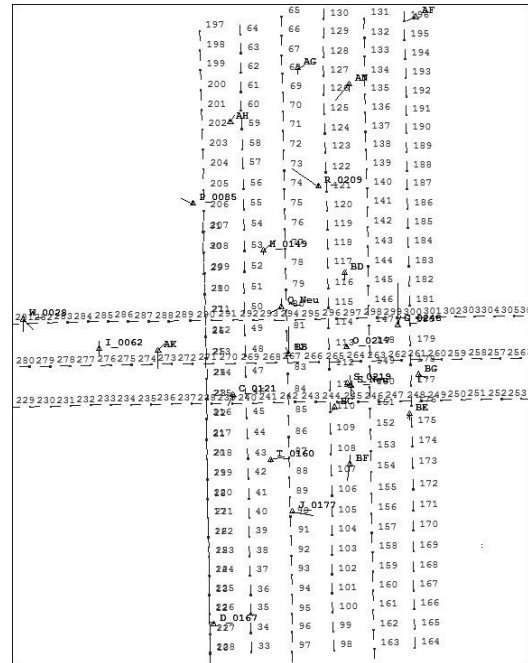


Fig. 9: Block layout of the UltraCam L test project (GSD 10cm @1000m AGL).

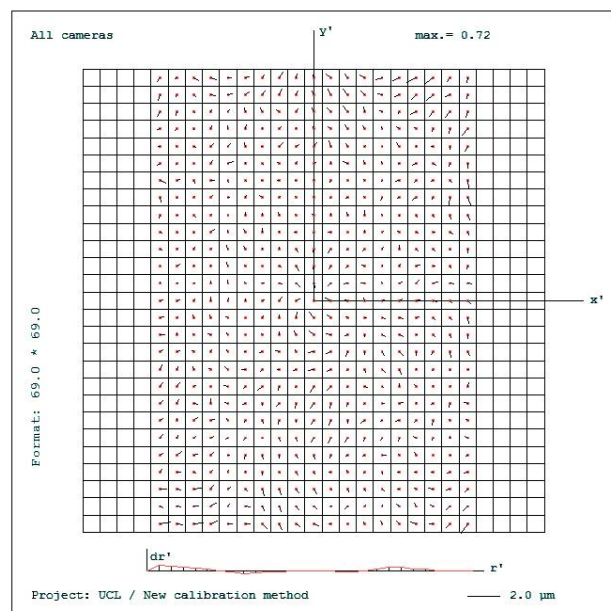
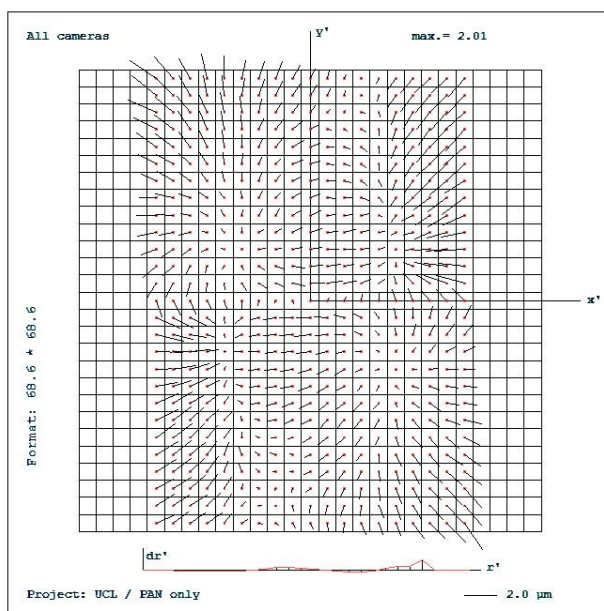


Fig. 10: Remaining image residuals after bundle adjustment. Left side: No colour tie points are used, no layer pre-correction. Right side: P/P and P/C tie points used, layer pre-correction (new calibration method) applied.

SELF CALIBRATION IN ULTRAMAP-AT

The UltraMap AT package adds the aero-triangulation functionality to the UltraMap software for all UltraCam camera products. Based on the huge set of self calibration parameters made available by BINGO (Kruck, 1984), UltraMap AT offers a selection of predefined parameters sets to the user:

1. No additional parameters
2. Radial symmetric distortions only
3. Special UltraCam parameter set
4. Advanced UltraCam parameter set

By choosing one of those four options, 0, 2, 23 or 61 additional parameters are determined in the bundle adjustment. If an experienced user wants to use a different set of parameters, there is also the possibility to manually edit the BINGO project file before BINGO is called.

CONCLUSION

We have illustrated the geometric camera calibration and post-processing concept for UltraCam digital aerial sensor systems. The focus was put on a new stitching concept using additional colour tie points in a free image mosaicking algorithm which has been implemented in the UltraMap software package. For the first time, we do not treat the camera calibration as absolutely error free in the stitching process but perform an optimal reconstruction of the inner orientation by using a technique known from free network adjustment. This even allows to validate the camera calibration by analysing the stitching results of a single (well textured) image.

The special importance of using a low resolution but monolithic reference channel (i.e. the green colour channel) to support high resolution PAN stitching was outlined for the UltraCam L camera system and verified in several test projects. The new stitching method is now available also for UltraCam X(p) systems (since UltraMap release v2.0).

The quality level of the entire post-processing process has been improved and we report a magnitude of remaining residuals of less than 1 μm in the image. The bundle solution of UltraMap AT is computed by means of a least squares adjustment technology based on the integrated

BINGO software product. Camera self calibration is also supported by UltraMap AT via predefined additional parameter sets.

REFERENCES

Gruber, M. & Ladstädter, R., 2006: *Geometric issues of the digital large format aerial camera UltraCamD*. International Calibration and Orientation Workshop EuroCOW 2006 Proceedings, 25-27 Jänner 2006, Castelldefels, Spanien.

Gruber, M. & Ladstädter, R., 2008: *Calibrating the digital large format aerial camera UltraCamX*. International Calibration and Orientation Workshop EuroCOW 2008 Proceedings, 30 January - 1 February 2008, Castelldefels, Spanien.

Gruber, M. & Wiechert, A., 2009: *New digital aerial cameras by Vexcel Imaging / Microsoft*, Proceedings of the Remote Sensing and Photogrammetry Society (RSPSoc) Annual Conference 2009, 8-11. 9. 2009, Leicester, UK.

Kröpfl, M. et al., 2004: *Geometric Calibration of the Digital Large Format Aerial Camera Ultracam_D*. The International Archives of Photogrammetry and Remote Sensing, VOL XXXV/1, p. 42 ff., July 2004, Istanbul, Turkey.

Kruck, E., 1984: *BINGO: Ein Bündelprogramm zur Simultanausgleichung für Ingenieurwissenschaften - Möglichkeiten und praktische Ergebnisse*, International Archive for Photogrammetry and Remote Sensing, Rio de Janeiro 1984.

Ladstädter R., 2007: *Softwaregestützte Kompensation temperaturabhängiger Bild-Deformationen für die Vexcel UltraCam*, Vorträge Dreiländertagung SGPBF, DGPF und OVG, Volume 16, p. 609-616, Basel 2007.

Leberl, F. et al., 2003: *The UltraCam Large Format Aerial Digital Camera System*, Proceedings of the American Society For Photogrammetry & Remote Sensing, 5-9 May, 2003, Anchorage, Alaska.

Meissl, P., 1962: *Die innere Genauigkeit eines Punkthaufens*, ÖZV, 50, pp. 159-165 and pp. 186-194.

Meissl, P., 1969: *Zusammenfassung und Ausbau der inneren Fehlertheorie eines Punkthaufens*, in: Beiträge zur Theorie der geodätischen Netze im Raum, DGK, A61, pp. 8-21, edited by K. Rinner, K. Killian and P. Meissl, BAW München.